Morphological characteristics and electrical properties analysis of silica based on river and coastal iron sand

Lalu Ahmad Didik Meiliyadi[1,2*], Muh. Wahyudi[1,2], Isniwana Damayanti[2], Ahmad Fudholi[3]

[1]Departement of Physics Education, Universitas Islam Negeri Mataram, Indonesia
[2]Advance Science and Integration Research Group, Universitas Islam Negeri Mataram, Indonesia
[3]Solar Energy Research Institute, Universiti Kebangsaan Malaysia, Malaysia

Corresponding Address: laludidik@uinmataram.ac.id

Article Info

ABSTRACT

This study aims to analyze silica's morphological characteristics and electrical properties based on the river and coastal sand. Iron samples were taken from Sompang river sand, East Lombok, and Coastal Sand from Gading, Mataram City. The silica was synthesized using the sol-gel method with a sintering temperature variation of 100 to 175 °C. Morphological characteristics samples analysis was done using SEM-EDX. The electrical properties of iron sand included measuring the dielectric constant using the parallel plate method. Furthermore, the resistivity was measured using the two-point probe method. In the silica-based on river sand sample, the resistivity value was inversely proportional to the sintering temperature. In contrast, the resistivity value of silica based on the coastal sand sample was directly proportional to the sintering temperature. Silica-based on river sand has a resistivity of about $7.1'10^4$ Ωm at a sintering temperature of 100°C and $3.5'10^4$ Ωm at a sintering temperature of 175°C. Silica-based on river sand has a resistivity of about $1.8'10^4$ Ωm at a sintering temperature of 100°C and $7.1'10^4$ Ωm at 175°C. This research is a preliminary study on the electrical properties of natural sand-based silica to improve understanding of the physical properties of silica to be used in technological applications, such as sensors. Furthermore, the dielectric constant value in the river sand sample was directly proportional to the sintering temperature. However, the dielectric constant in the coastal sand sample was inversely proportional to the sintering temperature. Silica-based on river sand has a dielectric constant of about $1.02'10^2$ at a sintering temperature of 100°C and $1.18'10^2$ at 175°C. Silica-based on coastal sand has a dielectric constant of about $1.97'10^2$ at a sintering temperature of 100°C and $1.15'10^2$ at 175°C.

INTRODUCTION

Indonesia has abundant natural resources. One of the natural resources found in mineral materials such as iron sand. Iron sand can generally be synthesized as an additive to cement and steel. In nanotechnology, iron sand is widely used as a catalyst, energy storage, magnetic data storage, ferrofluid, absorbent (Khan et al., 2021), and medical diagnosis (Satria et al., 2021).

Iron sand is also used in nanotechnology (Cheng & Zheng, 2022; Chundawat et al., 2022; Liu et al., 2022; Oktaviani et al., 2020). According to the source, there are three groups of iron sand, namely sea sand (sourced from the sea/beach), excavated sand (sourced from the soil), and river sand (sourced from rivers). Iron sand can be found in river sand, excavated sand, and coastal sand. Furthermore, iron sand contains magnetic minerals such as magnetite

(Fe_3O_4), maghemite ($\gamma - Fe_2O_3$), and hematite ($\alpha - Fe_2O_3$) (Didik et al., 2020; El-Feky et al., 2022; Liu et al., 2022).

Magnetite is more easily oxidized by air than maghemite and reaches a maximum amount when the temperature is raised to 220°C. This transformation continues to produce hematite which reaches its maximum at 320°C. This transformation will undoubtedly change the physical properties of magnetite as an adsorbent. Therefore, this conversion is essential in applying magnetite as an adsorbent (Sebayang et al., 2018).

The areas which has more iron sands in Indonesia is Lombok island (Asri et al., 2021; Pavlov et al., 2022; Susilawati et al., 2018). Lombok Island is located in the central part of Indonesia and has abundant natural resources. One of them is a mineral resource like silica sand situated in the eastern part of Lombok in the river and beach area (Dewi & Adi, 2018). Silica sand has many uses and can be used as the primary raw material in the glass industry (Gu et al., 2022; Pal et al., 2022; Wang et al., 2022; Zhang et al., 2022), cement (Mishra et al., 2017), ceramic mosaic (Puspitaningrum et al., 2017), ferrous silicon raw material, and sensor (Pal et al., 2022; Zheng et al., 2019). Until now, silica sand's potential in river and coastal sand has not been optimally utilized (Didik et al., 2021).

Coastal and river sand has not had many different characteristics and has almost the same content (Didik et al., 2021). However, the surrounding community has not fully utilized natural sand from the river because many people don't know the potential of iron sand. In general, difference between beach sand and river sand is shown in table 1.

Table 1. Comparison of physical properties of magnetic minerals based on river sand and beach sand (Didik et al., 2021).

Physical properties	Material magnetic based on Coastal sand	Material magnetic based on river sand
Colour	Darker	Dark
Morphology	Uniform particle size	Not uniform particle size

Physical properties	Material magnetic based on Coastal sand	Material magnetic based on river sand
Mineral magnetic percentage (%)	88.169	62.639
Fe content (mg/gram)	9.03	8.03

In previous studies, several methods of synthesizing river sand and coastal sand and their morphological and electrical characteristics have been found by using several methods, such as the coprecipitation method (Kurniawan et al., 2017), alkaline precipitation (Rianna et al., 2018), solid-state reaction (Malega et al., 2018), sol-gel (Fernández-Fernández et al., 2022; Vopel et al., 2017; Yan et al., 2022), coprecipitation sonication (Chen et al., 2016), and hydrothermal (Mishra et al., 2017). Mineral content and morphology characteristics were analyzed using X-Ray Fluorescence (XRF) (Rianto et al., 2018) and X-Ray Diffractometer (XRD) (Puspitaningrum et al., 2017), and Scanning Electron Microscope (SEM) (Malega et al., 2018).

However, there has been no research on the synthesis of iron sand nano silica based on river sand and coastal sand and its morphological and electrical characteristics, which are synthesized by the sol-gel method. Therefore, the researchers researched the synthesis of silica-based on river and coastal sand in Lombok Island and characterized the morphological and electrical characteristics.

METHODS

This research was carried out at UIN Mataram Physics Laboratory. The synthesis method used in this research was the Sol-Gel method (Hou et al., 2018; Pavlov et al., 2022). Iron sand samples were taken from Sompang river sand in East Lombok and Coastal Sand from Gading in Mataram City. Other research components were HCl solution with 12 M concentration Physical Analysis (99%) from Sigma Aldrich, NH₄OH solution with a concentration of 6,5 M PA (99%), and distilled water. The

morphological characteristic and mineral content were determined using SEM-EDX type Jeol JCM-7000.

Figure 1. Research Location

The samples were separated using permanent magnets and then sun-dried for four days. The samples were then oven-dried at 100°C for two hours after being washed four times using distilled water. The researchers sieved the iron sand sample using 200 mesh of sieve to separate the iron sand from impurities and other coarse components. The samples were synthesized using the sol-gel method. Ten grams of iron powder were dissolved into a 20 ml HCl solution with a 12 M concentration. The solution was stirred using a magnetic stirrer at 90 °C for 60 minutes. The samples were then dripped with a 6,5 M concentration of NH_4OH until the precipitate formed (Setiadi et al., 2018; Yu et al., 2022). The samples were then filtered with filter paper and washed four times using distilled water. They were dried in an oven at 100, 125, 150, and 175 °C. The chart of the experimental procedure of this research is shown in Figure 2.
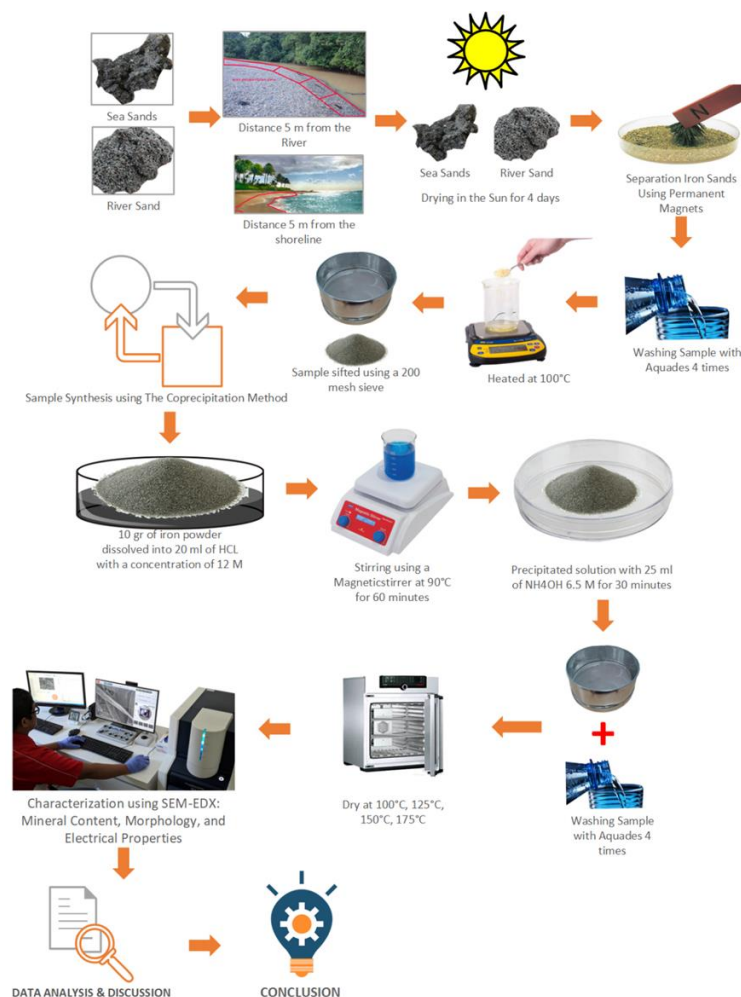

Figure 2. Experimental Procedure

Resistivity measured by using 2-probe points is shown in Figure 3. The CASSY 2 was used to measure the current and voltage values. This tool immediately displayed the current and voltage values on the CASSY 2 sensor. The equations to determine resistivities were 1 and 2 (Ningsih; et al., 2019).

$$R = \frac{V}{I} \tag{1}$$

$$\rho = R\frac{A}{L} \tag{2}$$

R is the electrical resistance of the iron sand (Ω), V is the applied input voltage (volts), I is the generated current (A), Ωm is the resistivity of silica, A is the cross-sectional area of the probe (m^2), and L is the distance between probes (m).
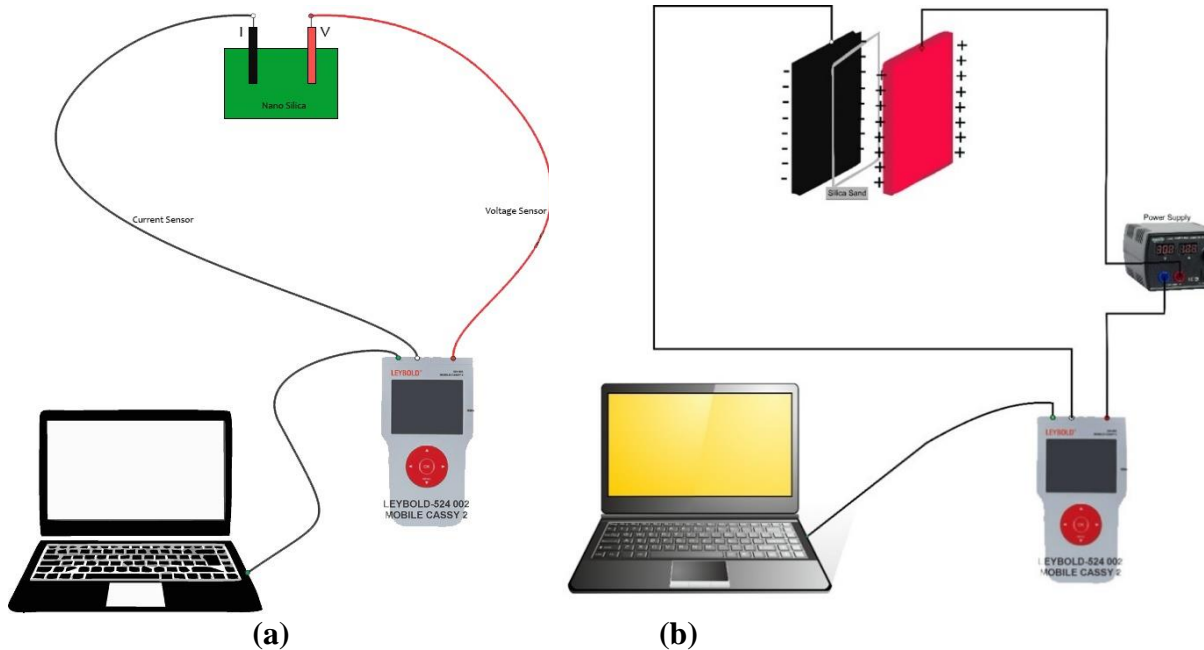

Figure 3. Instrument of silica based on iron sand electric properties measurement (a) two probe method for resistivity, (b) parallel plate for dielectricity

Dielectricity was measured by using parallel plates. The plates' size was 1.25 cm^2, and the distance between plates was 1 cm (Ningsih et al., 2019). The iron sand capacitance value was analyzed using equation 3, and the dielectric constant value was obtained using equation 4 (Ningsih; et al., 2019).

$$C = \frac{\varepsilon_o A}{d} \tag{3}$$

$$\varepsilon_r = C\frac{d}{\varepsilon_o A} \tag{4}$$

C is the capacitance of the iron sand (F), A is the plate area (m^2), ε_0 is the air permeability (8.85×10^{-12} F/m), d is the distance between the plates (m), and εr is the dielectric constant of the silica-based on iron sand.

RESULTS AND DISCUSSION

Silica-based on coastal sand and river sand mineral content was analyzed using EDX. Mineral content analysis results are shown in Table 1.

Based on Table 2, silica is the highest mineral content. Silica coastal sand content is (36.8 ±0.3) %, while silica river sand content

is (27.8±0.3) %. The intensity of the characteristic X-rays reflected as a result of EDX analysis is shown in Figure 4.

Table 2. Magnetic mineral content characteristics analyzed by EDX

| No | Element | Atomic percentage (%) | |
		Magnetic mineral based on Sompang River sand	Magnetic mineral based on Gading Sand
1	C	8,4±0,3	15,8±0,5
2	O	40.3±0,6	32,5±0,5
3	Na	2,8±0,1	1,1±0,1
4	Fe	3,1±0,2	3,0±0,2
5	Ca	1,1±0,1	1,3±0,1
6	Si	27,8±0,3	36,8±0,3
7	K	3,5±0,1	1,2±0,2
8	Al	7,3±0,2	7,9±0,2
9	Ti	0,3±0,1	0,4±0,1
10	Mg	0,4±0,1	0,3±0,1

The river's and coastal sand morphological characteristics were analyzed at UIN Mataram using Scanning Electron Microscope type Jeol JCM-7000. The morphological characteristics of silica based on coastal iron sand samples sintered at a temperature of 100°C are shown in Figure 5.

Figure 5 shows the morphological characteristics of silica-based coastal iron sand sintered at 100°C. Figure 5 (a) is the result of SEM with a magnification of 2500x, while Figure 5 (b) is a diagram of the percentage distribution of grain sizes of silica based on coastal iron sand samples. The distribution of grain sizes silica based on coastal sand samples 70% has grain size 0-3 μm, 3-6 μm has a percentage of 10%, and 20% has grain size 6-10 μm. The morphological characteristics of silica based

on river sand samples sintered at a temperature of 100°C are shown in Figure 6.

Figure 6 shows the silica-based river sand sample morphological characteristics sintered at a temperature of 100°C. Figure 6 (a) shows the result morphological characteristic of silica based on river sand analyzed using SEM with a magnification of 2500x. Figure 6 (b) is a diagram of the percentage distribution of grain size of the silica-based river sand sample sintered at a temperature of 100°C. The distribution of grain sizes silica based on river sand samples 14,29% has grain size 10-50 μm, 50-100 μm has a percentage of 21,43%, 28,56% has grain size 100-200 μm and grain size 200-250 μm with 14,29% percentage. The distribution of silica grains based on coastal sand is more uniform than that of grains based on river sand. This is indicated by the greater variation in grain size percentage of silica based on river sand (figure 6b) compared to silica based on coastal sand (figure 5b).

Table 3. The average grain size of silica is based on river sand and coastal sand

| Sintering Temperature (°C) | Average grain size (μm) | |
	Silica-based on Coastal sand	Silica-based on river sand
100	3,148	121,299
175	107,135	77,663

Morphological characteristics Analysis of silica based on river sand and coastal sand using SEM shows the average grain size. The average grain size of the results of the SEM analysis is shown in Table 3.
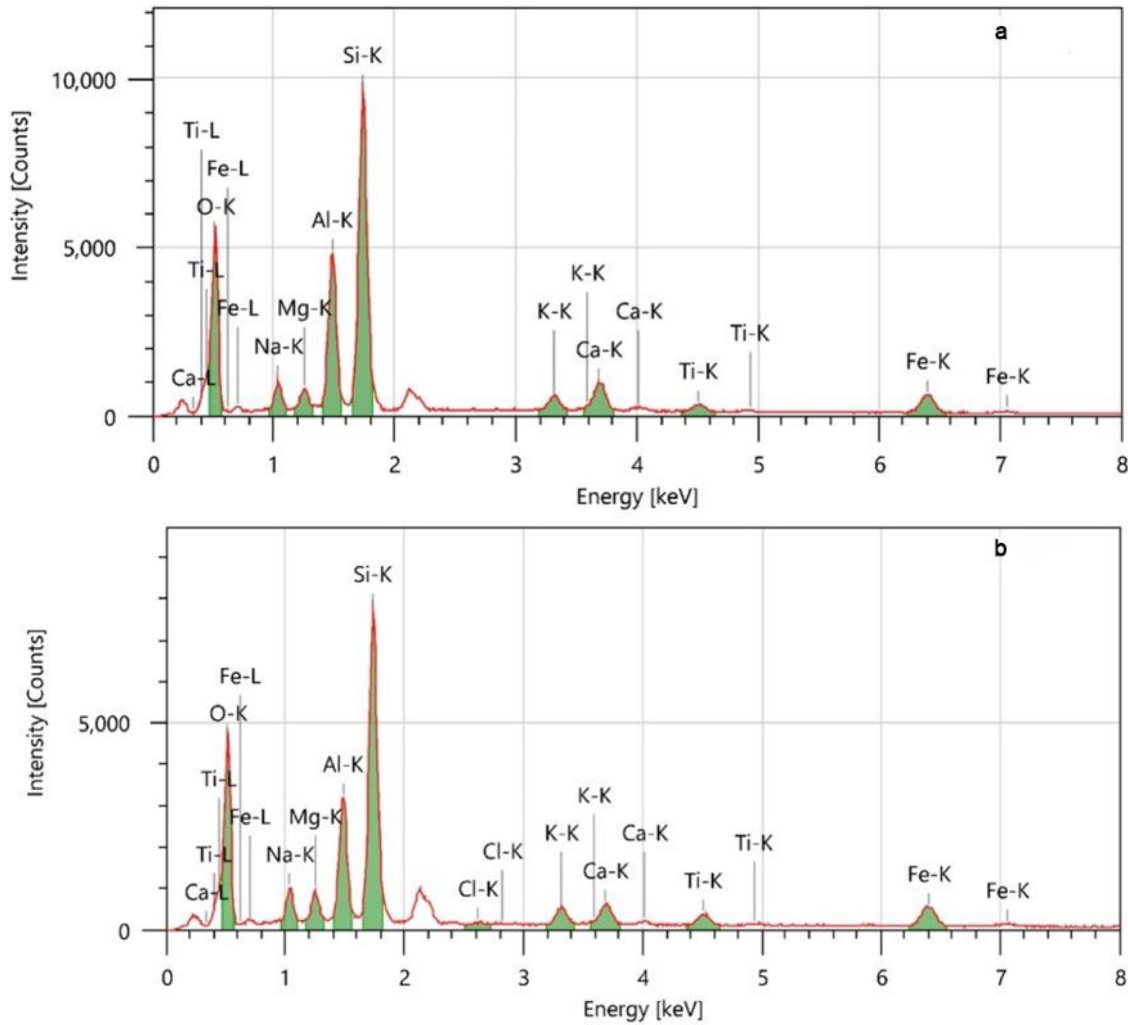
Figure 4. Minerals content analysis spectrum measured using EDX on (a) coastal sand from Gading Beach and
(b) river sand from Sompang River

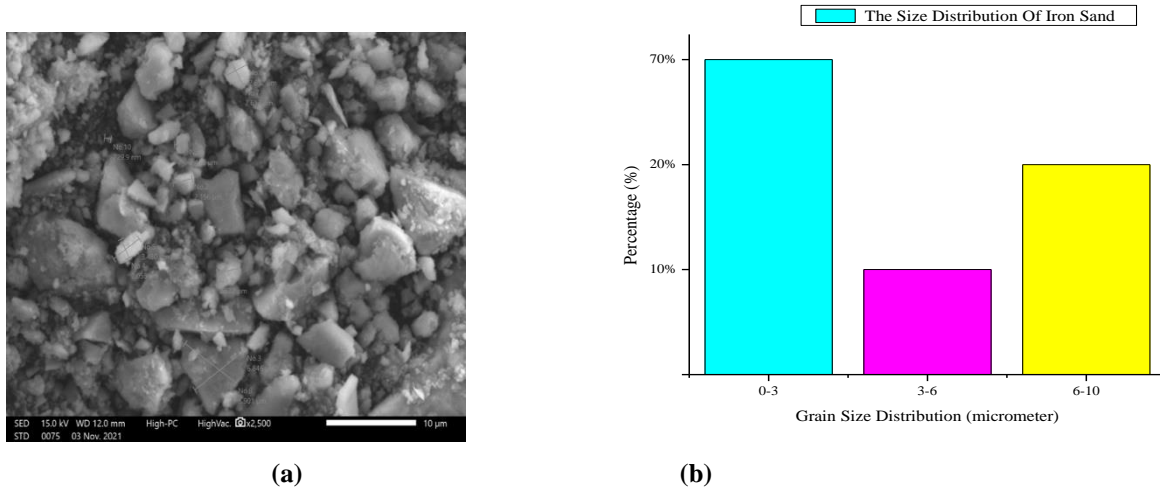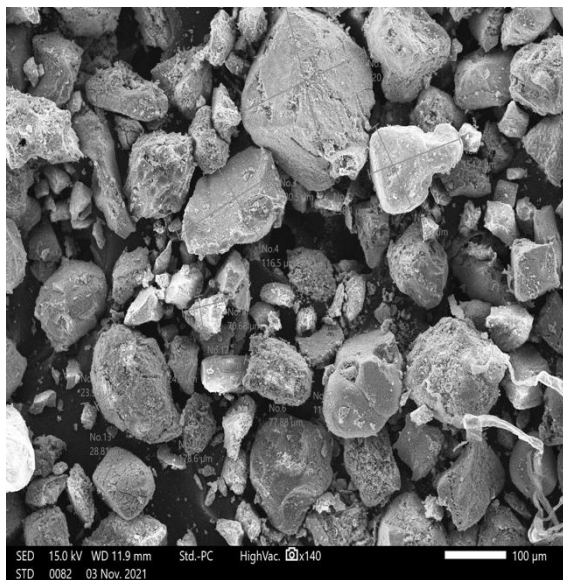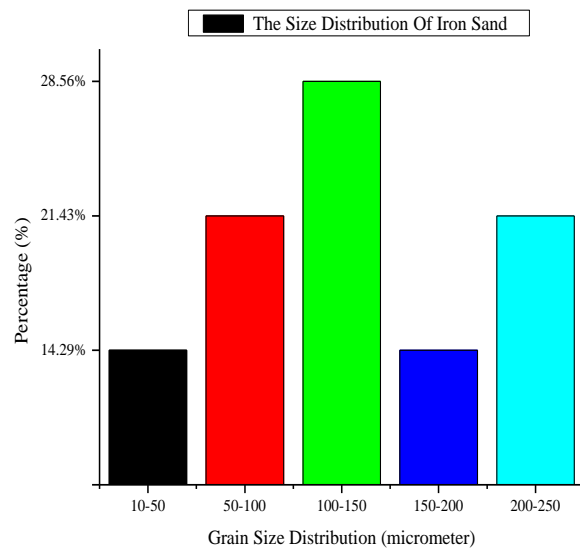| (a) | (b) |

Figure 5. Morphological Characteristics of silica based on Coastal Sand Samples at sintering Temperature of
100°C; (a) SEM Results with 2500x Magnification, (b) Percentage Distribution of Grain Sizes of Costal
Iron Sand

Figure 6. Morphological Characteristics of silica based on River Sand Samples at sintering Temperature of 100°C; (a) SEM results with a magnification of 2500x, (b) Percentage of Grain Size Distribution of River Iron Sand

Based on table 3, the average grain size of silica based on coastal sand is 3.148 μm with an average grain size of 107.135 μm at a sintering temperature of 175°C. The silica-based on river sand's average grain size is 121,299 μm at a temperature of 100°C, and the average grain size of silica is 77.663 μm at a sintering temperature of 175°C.

From the average grain size of the river iron sand sample and the coastal iron sand sample obtained, the grain size of the silica-based on the coastal sand sample at 100°C is smaller than the sample size at 175°C. While silica is based on river sand samples, the grain size sample at 100°C is larger than the grain size at 175°C.

Silica-based on iron sand was analyzed using SEM showed that the silica-based on coastal sand has a uniform particle size compared to silica based on river sand. The magnetic mineral particle size of silica based on iron sand is also smaller than the magnetic particle size of silica based on river sand. Beach sand has a much finer size than river sand (Asri et al., 2021; Shaheen et al., 2022). This is caused by beach sand deposits formed by seawater wave sediments. It is caused beach sand has a smoother structure. At the same time, limestone deposits fine grains and coarse structures caused river sand sediment.

Resistivity is a material characteristic that can indicate the ability of the material to conduct electric current (Didik & Wahyudi, 2020; Ningsih; et al., 2019). Resistivity is a basic parameter to characterize the physical properties possessed by a material, namely the ability to pass an electric current. The greater the resistivity value of a material, the more difficult it is for the material to conduct an electric current (Luo et al., 2022). If the rock is getting stronger and it is difficult for electric current to pass, then the amount of resistance given by the rock is getting bigger.

The dielectric constant is a material characteristic that indicates the ability of the material to make polarization. In simple terms, the magnitude of the electric polarization is caused by four sources, namely, the electronic component caused by the induced field in the electron cloud that surrounds each atom in a material (Didik et al., 2020). Second, the ionic contribution is associated with the relative motion of cations and anions in an electric field. Third, orientational polarization is due to the rotation of the molecular dipole in the field.

Besides, the source of material polarization is also caused by the movement of charge carriers, namely the movement of ions or electrons under the influence of a field. Silica-based on iron sand electrical properties showed in Figure 7.

Figure 7 (a) shows that the sintering temperature is inversely proportional to the resistivity value obtained at silica based on river sand. The lower the sintering temperature of the silica-based on river iron sand sample used, the higher the resistivity value of the iron sand sample obtained. Silica-based river sand has a resistivity of about $7.1'10^4$ Ωm at a sintering temperature of $100°C$ and $3.5'10^4$ Ωm at a temperature of $175°C$. While in the silica-based coastal iron sand sample shown in Figure 7 (b), the resistivity value is directly proportional to the sintering temperature of the iron sand sample. Silica-based river sand has a resistivity of about $1.8'10^4$ Ωm at sintering temperature $100°C$ and $7.1'10^4$ Ωm at temperature $175°C$. The higher sintering temperature of the sample was used. The greater resistivity value of the sample was obtained. It can be affected by the physical properties of silica-based on iron sand, such as dielectric constant and other mechanical properties of the material's particle size.

From the results of the measurement of silica based on the river sand dielectric constant shown in Figure 7 (a), the higher the sintering temperature used, the greater the value of the dielectric constant obtained. At the same time, the value of the dielectric constant in the sample of coastal iron sand showed in Figure 7 (b). Based on Figure 7 (b), the higher the sintering temperature, the smaller the dielectric constant value obtained. Silica-based on river sand has a dielectric constant of about $1.02'10^2$ at sintering temperature $100°C$ and $1.18'10^2$ at temperature $175°C$, while silica based on coastal sand has a dielectric constant of about $1,97'10^2$ at sintering temperature $100°C$ and $1.15'10^2$ at temperature $175°C$. It can be concluded that in the silica-based on river iron sand sample, the temperature is directly proportional to the dielectric constant value. In contrast, in the silica-based on coastal iron sand sample, the temperature is inversely proportional to the dielectric constant value obtained.
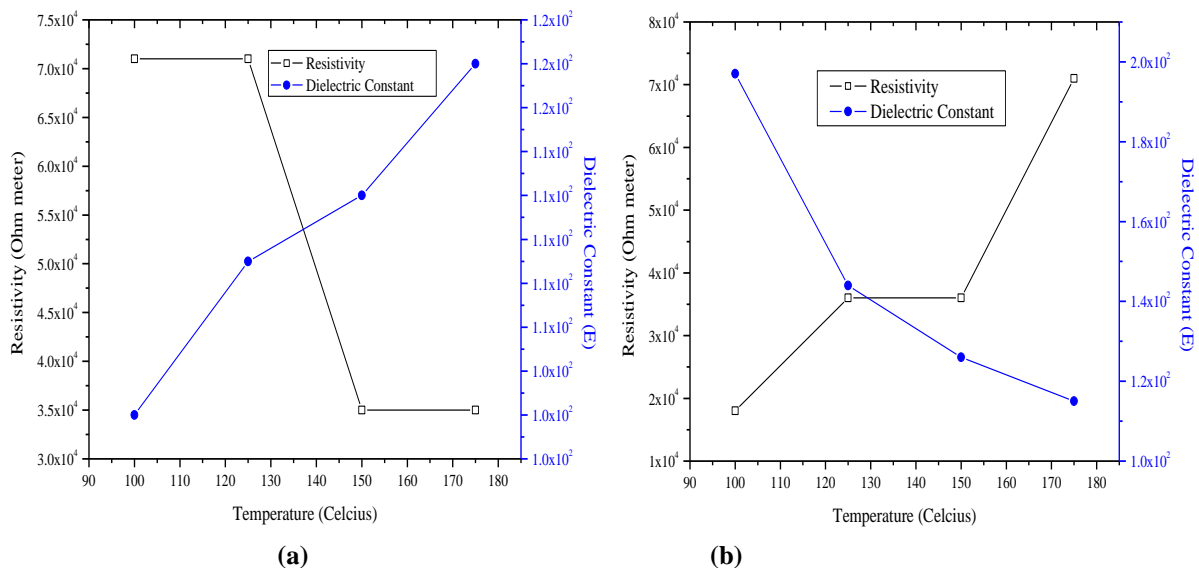

                (a)   **(b)**

Figure 7. Relationship between electrical temperatures of silica based on (a) river iron sand and (b) coastal iron sand

The grain size of silica will affect the dielectric constant and resistivity value. The smaller the grain size of the material (silica based on iron sand sample), the greater the resistivity value. The smaller grain size of the sample will make electrons hard to move, so

the resistivity will increase (Nugraha et al., 2016). The smaller grain size of the sample will increase the capacitance value, followed by increasing the dielectric constant value. The greater dielectric constant value made the material's ability to store electrical energy greater. The dielectric constant value is caused by the presence of different contents in each sample (Zhaoa et al., 2022). It is caused by the capacitance value being directly proportional to the dielectric constant value (Kurniawan et al., 2017).

Capacitors are devices used to store dielectricity-based energy. The energy stored in the capacitor is shown in equation 5.

$$E = \frac{1}{2} CV^2 \tag{5}$$

C is the capacitance (farads), and V is the potential difference applied to the capacitor (volts). Based on equation 4, the capacitance is proportional to the dielectric constant. In equation 5, it appears that the energy is proportional to the capacitance, so it can be concluded that the greater the dielectric constant, the greater the energy stored in the capacitor.

CONCLUSION AND SUGGESTION

Based on the results of this research showed that the characteristics of silica based on river sand and coastal sand are different. Silica-based on river sand has a granular shape that is not fine (coarser than the shape of coastal sand grains) and has not too large grain size because river sand usually comes from hard and sharp river rocks. While silica based on coastal sand has the characteristics of fine grains and is smaller than river sand. In the silica-based on river sand sample, the resistivity value is sintering temperature inversely. In contrast, in the silica-based on coastal sand, the resistivity value is proportional to the sintering temperature. Silica-based on the river sand sample's dielectric constant value is proportional to the sintering temperature. In contrast, in the silica-based coastal sand sample, the dielectric constant is inverse to the sintering temperature.

AUTHOR CONTRIBUTIONS

LA provides ideas for conducting research, AF makes research designs, MW collects data and analyzes it, and LA and ID write discussions and conclusions.

REFERENCES

Asri, L., Didik, L. A., & Bahtiar, B. (2021). Sintesis dan analisis kandungan mineral dan karakteristik sifat listrik nanopartikel pasir besi pantai Telindung kabupaten Lombok Timur. *JST (Jurnal Sains Dan Teknologi)*, *10*(1), 85–91. https://doi.org/10.23887/jst-undiksha.v10i1.22765

Chen, Q., Xu, S., Liu, Q., Masliyah, J., & Xu, Z. (2016). QCM-D study of nanoparticle interactions. *Advances in Colloid and Interface Science*, *233*(2), 94–114. https://doi.org/10.1016/j.cis.2015.10.004

Cheng, Y., & Zheng, L. (2022). Engineering silica encapsulated composite of acyltransferase from Mycobacterium smegmatis and MIL-88A: A stability- and activity-improved biocatalyst for N-acylation reactions in water. *Colloids and Surfaces B: Biointerfaces*, *217*, 112690. https://doi.org/10.1016/j.colsurfb.2022.112690

Chundawat, N. S., Parmar, B. S., Deuri, A. S., Vaidya, D., Jadoun, S., Zarrintaj, P., Barani, M., & Chauhan, N. P. S. (2022). Rice husk silica as a sustainable filler in the tire industry. *Arabian Journal of Chemistry*, *15*(9), 104086. https://doi.org/10.1016/j.arabjc.2022.104086

Dewi, S. H., & Adi, W. A. (2018). Synthesis and characterization of high purity Fe 3 O 4 and α - Fe 2 O 3 from local iron sand. *Journal of Physics: Conference*

Series, *1091*(1). https://doi.org/10.1088/1742-6596/1091/1/012021

Didik, L. A., Aini, H., & Zohdi, A. (2020). Analisis perbandingan kandungan fe dan karakteristik sifat listrik pasir besi sungai dan pantai. *Jurnal Fisika Flux: Jurnal Ilmiah Fisika FMIPA Universitas Lambung Mangkurat*, *17*(2), 138–145. https://doi.org/http://dx.doi.org/10.20527/flux.v1i1.7689

Didik, L. A., Damayanti, I., Jumliati, J., & Alfadia Lestari, P. D. (2021). Morphological characteristics and mineral content analysis of magnetic minerals based on river and coastal sand using SEM-EDX. *Jurnal Sains Dasar*, *10*(2), 44–50. https://doi.org/10.21831/jsd.v10i2.42217

Didik, L. A., & Wahyudi, M. (2020). Analisa kandungan fe dan karakteristik sifat listrik pasir besi pantai telindung yang disintesis dengan beberapa metode. *Indonesian Physical Review*, *3*(2), 64–71. https://doi.org/10.29303/ipr.v3i2.58

El-Feky, M. S., Mohsen, A., El-Tair, A. M., & Kohail, M. (2022). Microstructural investigation for micro - nano-silica engineered magnesium oxychloride cement. *Construction and Building Materials*, *342*, 127976. https://doi.org/10.1016/j.conbuildmat.2022.127976Get rights and content

Fernández-Fernández, M., Á. C., & M., M. (2022). Molecular simulation of methane hydrate growth confined into a silica pore. *Journal of Molecular Liquids*, *362*, 119698. https://doi.org/10.1016/j.molliq.2022.119698

Gu, Y., Wang, L., Chen, J., Jiang, Z., Zhang, Y., Wang, W., Chen, H., Shen, J., Zhong, J., Meng, S., Li, J., Zhu, Y., & Sun, T. (2022). Surface acidity of colloidal silica and its correlation with sapphire surface polishing. *Colloids and Surfaces A: Physicochemical and Engineering Aspects*, *651*, 129718. https://doi.org/10.1016/j.colsurfa.2022.129718

Hou, X., Wang, X., & Mi, W. (2018). Progress in Fe3O4-based multiferroic heterostructures. *Journal of Alloys and Compounds*, *765*, 1127–1138. https://doi.org/10.1016/j.jallcom.2018.06.287

Khan, J., Lin, S., Nizeyimana, J. C., Wu, Y., Wang, Q., & Liu, X. (2021). Removal of copper ions from wastewater via adsorption on modified hematite (α-Fe2O3) iron oxide coated sand. *Journal of Cleaner Production*, *319*, 128687. https://doi.org/10.1016/j.jclepro.2021.128687

Kurniawan, C., Eko, A. S., Ayu, Y. S., Sihite, P. T. A., Ginting, M., Simamora, P., & Sebayang, P. (2017). Synthesis and characterization of magnetic elastomer based PEG-Coated Fe3O4 from natural iron sand. *IOP Conference Series: Materials Science and Engineering*, *202*(1). https://doi.org/10.1088/1757-899X/202/1/012051

Liu, G., Liu, B., Liu, K., Zhai, G., & Guo, Z. (2022). Silica crystallinity: Characteristics and controlling factors in marine shale of the upper Yangtze area, China. *Marine and Petroleum Geology*, *143*, 105833. https://doi.org/10.1016/j.marpetgeo.2022.105833

Luo, K., Luo, Y., Liu, Y., Zhang, Y., Chen, W., Bai, Z., & Tang, S. (2022). Hydrophobic and hydrophilic selectivity of a multifunctional carbonyldiimidazolium/dodecyl modified silica stationary phase. *Journal of Chromatography A*, *1677*, 463300. https://doi.org/10.1016/j.chroma.2022.463300

Malega, F., Indrayana, I. P. T., & Suharyadi, E. (2018). Synthesis and characterization of the microstructure and functional group bond of fe3o4

nanoparticles from natural iron sand in Tobelo North Halmahera. *Jurnal Ilmiah Pendidikan Fisika Al-Biruni*, *7*(2), 129. https://doi.org/10.24042/jipfalbiruni.v7i2.2913

Mishra, S., Dey, K., Chowdhury, U., Bhattacharya, D., Ghosh, C. K., & Giri, S. (2017). Multiferroicity around Verwey transition in Fe3O4 thin films. *AIP Advances*, *7*(12). https://doi.org/10.1063/1.5011119

Ningsih, F., Fitrianingsih, & Didik, L. A. (2019). Analisis pengaruh lama penggerusan terhadap resistivitas dan konstanta dielektrik pada pasir besi yang disintesis dari kabupaten Bima. *Indonesian Physical Review*, *2*(3), 92–98. https://doi.org/10.29303/ipr.v2i3.31

Nugraha, P. A., Sari, S. P., Hidayati, W. N., Dewi, C. R., & Kusuma, D. Y. (2016). The origin and composition of iron sand deposit in the southern coast of Yogyakarta. *AIP Conference Proceedings*, *1746*(June 2016). https://doi.org/10.1063/1.4953953

Oktaviani, E., Nasri, M. Z., & Deswardani, F. (2020). Sintesis dan karakterisasi nanopartikel Fe3o4 (Magnetite) dari pasir besi sungai Batanghari Jambi yang dienkapsulasi dengan polyethylene glycol (Peg-4000). *Jurnal Pendidikan Fisika …*, *8*(3), 97–103.

Pal, P., Li, H., & Saravanamurugan, S. (2022). Removal of lignin and silica from rice straw enhanced accessibility of holocellulose for the production of high-value chemicals. *Bioresource Technology*, *361*, 127661. https://doi.org/10.1016/j.biortech.2022.127661

Pavlov, V. S., Bruter, D. V., Konnov, S. V., & Ivanova, I. I. (2022). Effect of silica source on zeolite MFI crystallization in fluoride media and its physicochemical and catalytic properties. *Microporous and Mesoporous Materials*, *341*, 112088. https://doi.org/10.1016/j.micromeso.2022.112088

Puspitaningrum, A., Taufiq, A., Hidayat, A., Sunaryono, Hidayat, N., & Samian. (2017). Optical properties of Fe3O4 magnetic fluid from iron sand. *IOP Conference Series: Materials Science and Engineering*, *202*(1), 0–9. https://doi.org/10.1088/1757-899X/202/1/012054

Rianna, M., Sembiring, T., Situmorang, M., Kurniawan, C., Setiadi, E. A., Tetuko, A. P., Simbolon, S., Ginting, M., & Sebayang, P. (2018). Characterization of natural iron sand from Kata Beach, West Sumatra with high energy milling (Hem). *Jurnal Natural*, *18*(2), 97–100. https://doi.org/10.24815/jn.v18i2.11163

Rianto, D., Yulfriska, N., Murti, F., Hidayati, H., & Ramli, R. (2018). Analysis of crystal structure of Fe3O4 thin films based on iron sand growth by spin coating method. *IOP Conference Series: Materials Science and Engineering*, *335*(1). https://doi.org/10.1088/1757-899X/335/1/012012

Satria, B., Silvia, Z. M., & Fajar, J. (2021). Magnetic susceptibility and grain size distribution as prospective tools for selective exploration and provenance study of iron sand deposits: A case study from Aceh, Indonesia. *Heliyon*, *7*, e08584. https://doi.org/10.1016/j.heliyon.2021.e08584

Sebayang, P., Kurniawan, C., Aryanto, D., Setiadi, E. A., Tamba, K., Djuhana, & Sudiro, T. (2018). Preparation of Fe3O4/Bentonite nanocomposite from natural iron sand by coprecipitation method for adsorbents materials. *IOP Conference Series: Materials Science and Engineering*, *316*(1). https://doi.org/10.1088/1757-899X/316/1/012053

Setiadi, E. A., Yunus, M., Nababan, N., Simbolon, S., Kurniawan, C., Humaidi, S., Sebayang, P., & Ginting, M. (2018). The effect of temperature on synthesis

of MgFe2O4 based on natural iron sand by Coprecipitation method as adsorbent Pb ion. *Journal of Physics: Conference Series*, *985*(1). https://doi.org/10.1088/1742-6596/985/1/012046

Shaheen, M. E., Gagnon, J. E., & Fryer, B. J. (2022). Morphological and ablation characteristics of brass and fused silica after interaction with ArF excimer laser. *Optik*, *262*, 169388. https://doi.org/10.1016/j.ijleo.2022.169388

Susilawati, Doyan, A., Wahyudi, Gunawa, E. R., Kosim, Fithriyani, A., & Khair, H. (2018). Identifikasi kandungan fe pada pasir besi alam di Kota Mataram. *Jurnal Pendidikan Fisika Dan Teknologi*, *4*(1), 105–110.

Vopel, K., Pook, C., Wilson, P., & Robertson, J. (2017). Offshore iron sand extraction in New Zealand: Potential trace metal exposure of benthic and pelagic biota. *Marine Pollution Bulletin*, *123*(1–2), 324–328. https://doi.org/10.1016/j.marpolbul.2017.09.018

Wang, D., Chen, X., Feng, J., & Sun, M. (2022). Recent advances of ordered mesoporous silica materials for solid-phase extraction. *Journal of Chromatography A*, *1675*, 463157. https://doi.org/10.1016/j.chroma.2022.463157

Yan, F., Tong, L., Qin, H., Guo, W., Liu, J., Xie, W., Gao, P., & Xiao, H. (2022). Controlled synthesis of biomimetic materials with protruding structures by in situ growth of silica nanorods via hydroxyl-localized droplet template

method. *Colloids and Surfaces A: Physicochemical and Engineering Aspects*, *651*, 129705. https://doi.org/10.1016/j.colsurfa.2022.129705

Yu, S., Tang, Z., Wu, S., & Guo, B. (2022). Use of naturally small molecule as an intelligent interfacial modifier for strengthening and toughening silica-filled rubber composite. *Composites Science and Technology*, *227*, 109624. https://doi.org/10.1016/j.compscitech.2022.109624

Zhang, C., Yu, S., Tang, Z., & Guo, B. (2022). Catalyzed silanization by supporting ceria on silica towards rubber composites with improved mechanical properties. *Composites Communications*, *32*, 101168. https://doi.org/10.1016/j.coco.2022.101168

Zhaoa, F., Jina, J., Hua, G., Mab, C., Lua, L., Hub, T., Liu, Y., Wei, D., Ming, H., Jia, L., & Chun-Lin. (2022). Energy storage performance of silicon-integrated epitaxial lead-free BaTiO3-based capacitor. *Chemical Engineering Journal*, *450*(3), 138312. https://doi.org/10.1016/j.cej.2022.138312

Zheng, W. C., Zheng, D. X., Wang, Y. C., Li, D., Jin, C., & Bai, H. L. (2019). Flexible Fe3O4/BiFeO3 multiferroic heterostructures with uniaxial strain control of exchange bias. *Journal of Magnetism and Magnetic Materials*, *481*, 227–233. https://doi.org/10.1016/j.jmmm.2019.02.068